The ThermoSnooker Simulation: a computational analysis of gases

Stefano Veroni, 11/12/2020

***Abstract* — A python-based simulation was created to investigate both the microscopic and macroscopic properties of gases. As theoretically expected, momentum, energy and angular momentum were conserved. Besides, the speed distribution was demonstrated to conform to Maxwell Boltzmann curve. Macroscopically, it was shown Van der Waal model provides a better description of gases than the Ideal Gas equation of state, and its b factor was estimated. Finally, properties of a mixture of gases were also investigated.**

I. Introduction

THIS report describes the techniques implemented to simulate and analyse a gas in python and discusses the results of such analysis.

A graphical presentation of the simulation based on the classes Ball and Simulation, whose main attributes and methods are outlined in the computing script (tasks 2 to 6)[1], can be observed in Fig 1.1.

The initialization of the simulation was randomized as much as possible, as a grid of all the possible positions where the balls could spawn was first created, and then the positions were randomly picked. The velocities of the balls were randomly assigned too. This improved the efficiency of the simulation, as it then required much less frames to reach a random homogeneous distribution of the particles and their velocities.

The conventions about symbols and values used in the investigations are presented in table 1.

TABLE I

Quantity	Symbol	Value
Radius of the balls	R_b	$1.0 \cdot 10^{-3}$ kg
Mass of the balls	m_b	$1.0 \cdot 10^{-3}$ m
Number of balls	N	varies
Radius of the container	R_c	varies
Binned Distribution Width	w	varies

II. Analysis of the Microscopic Properties of the Gas simulation

A. Distance from Centre and Inter-balls Separation

In this section, the results obtained in the analysis of the microscopic properties of the particles are outlined and discussed. These are position, velocity, momentum, angular momentum and kinetic energy. In order to perform a statistically significant analysis, a relatively big number of balls (2000) and of frames (20000) were implemented.

The distribution of the balls from the centre of the container is described in Fig 2.1. It can be seen it increases linearly. The theoretical curve to which it is compared represents the predicted number N_r of balls whose distance r from centre is comprised between $r - \frac{w}{2}$ and $r + \frac{w}{2}$:

$$N_r(r) = \frac{2w}{R_c^2} rN. \tag{2.1}$$

This prediction can easily be shown following the assumption the balls are homogeneously distributed in the container, in fact, assuming their density is

$$\rho = \frac{N}{\pi R_c^2}, \tag{2.2}$$

then $N_r(r)$ is

$$N_r(r) = \int_{r'=r-\frac{w}{2}}^{r'=r+\frac{w}{2}} \int_{\phi=0}^{\phi=2\pi} \rho \, r' \, d\phi \, dr', \tag{2.3}$$

which ultimately results in Eq 2.1. As expected, the distribution and the theoretical prediction match. The following plot, Fig 2.2, shows the inter-ball separation.

B. Energy, Momentum and Velocity

Let's now consider the kinetic energy, in Fig 2.3. It can be seen to be conserved throughout the simulation: this should represent no surprise, as, since the container was approximated having infinite mass, it should have been so. Besides the code itself would have interrupted the simulation if it happened not to be so: then, instead of plotting the value of the kinetic energy as calculated after each frame of the simulation, I decided just to plot a straight line with the ordinate being equal to its initial value.

Similarly, Fig 2.4 confirms angular momentum is conserved. However, a slightly zigzagged characteristic can be observed. I assume, as it was recalculated after each step, it is a consequence of the floating-point arithmetic (FPA) python is based on.

Analogous considerations hold for the sum of the magnitudes of the balls: as the container's mass is infinite, and the collisions are elastic, the overall sum of the magnitudes of momenta is conserved, and it can be observed in plot d in Fig 2.5, net of FPA-derived slightly zigzagged shape. Plots a, b, c, instead, respectively display the evolution of the sum of the x and y components of momenta and of momenta itself over time. They can be seen to slightly oscillate in time: besides the FPA, this is due the fact when a ball bounces against the container, its radial velocity is reversed. The oscillations occur around zero: this means the velocities are uniformly distributed.

This can be appreciated in Fig 2.6, where the x-velocity, y-velocity and speed distributions are plotted as they are at

the end of the simulation. The number of bins was chosen following Freedman-Diaconis rule [2]. The distributions perfectly match the corresponding theoretical curves, i.e. a gaussian of form

$$f(v_z) = \sqrt{\frac{m_b}{2\pi k_b T}}\, e^{-\frac{m_b v_z^2}{2k_b T}}\, Nw, \tag{2.6}$$

where k_b is Boltzmann's constant, for the x and y components of velocities, and the 2D Maxwell-Boltzmann distribution for the speeds:

$$f_{MB}(v) = \frac{m_b\, v}{k_b T}\, e^{-\frac{m_b v^2}{2k_b T}}\, Nw. \tag{2.7}$$

Finally, let's consider another simulation, which had exactly the same parameters as the previous one apart the velocities, which were boosted in the x direction of 1.5 m/s. As it can be seen in Fig 2.7, after a major oscillation, equilibrium is eventually reached, although, as it could be expected, it required more time.

III. Analysis of a Mixture of Multiple Gas Species

The code was also enhanced to support multiple species of gases contemporarily. Then, additional analysis was carried out: the distance from the centre and the velocity/speed distributions of such mixture, as displayed in Fig 3.1 and 3.2 were shown to both follow the distributions described in section II, even if the latter does not perfectly match, due to the smaller number of frames run, i.e. 6000.

Finally, Dalton's Law of partial pressures was investigated and confirmed: as Fig. 3.3 shows, the total pressure is the sum of the partial ones each specie exerts.

IV. Analysis of the Macroscopic Properties of the Gas simulation

In this section, the relation between the simulation's state variables pressure P, volume V, temperature T and number of balls N is explored. The reader should observe that, as this is a 2D simulation, the volume is bidimensional, area has dimensions of length, pressure of Pa · m. The starting point of the analysis is the ideal gas equation of state

$$PV = Nk_b T \tag{4.1}$$

88 simulations were run for 50,000 frames. 24 (the ones for the P-N relation, Fig 4.4) for 100,000 frames. This choice was made after some rough analysis showed "large-N slow pressure convergence (LSPC)": for large Ns, it requires longer time for the pressure to converge to its exact value, i.e. the one it would have after infinite time.

Figures 4.1 and 4.2 confirm that the pressure linearly increases with temperature. However, it can be seen, especially if the volume occupied by the balls is relatively big, hence as the container's volume is small (Fig 4.1) or the number of balls is big (Fig 4.2), that the gradient of the plot is bigger than the ideal gas low predicts.

Fig 4.3 confirms pressure is inversely proportional to volume.

Finally, Figure 4.4, disproves the concept pressure is directly proportional to the number of balls: this is evident, in fact, for large N and small container's volumes.

Let's now consider Van der Waal's equation of state

$$\left(P + a\frac{N^2}{V^2}\right)(V - Nb) = Nk_B T, \tag{4.2}$$

where the a factor accounts for the reciprocal attraction or repulsion, while the b factor accounts for the volume the particles occupy. As in our simulation the particles don't interact between each other, apart during collisions, a is set to zero. Then Eq 4.2 can be equivalently rearranged, depending on the quantity we focus on, as

$$P = \frac{Nk_b T}{V - Nb}, \tag{4.3}$$

$$b = \frac{V}{N} - \frac{k_B T}{P}. \tag{4.4}$$

As b accounts for the volume occupied by the balls, it was assumed being directly proportional to their volume, then:

$$b = b'\pi R_b^2. \tag{4.5}$$

For each of the 112 simulations run, a certain value of b' was calculated from Eq 4.4 and Eq 4.5, then the average was taken. It was noted that, for big Ns the value for b' sometimes resulted smaller than 0.5: such values were discarded from the averaging process, being attributed to LSPC. The result of the average was:

$$b' = 2.1 \pm 0.6. \tag{4.6}$$

Such value was then used in Eq 4.3 to produce Figures 4.5, 4.6, 4.7 and 4.8. As it is shown, Van der Waal's equation represents a much better fit of the simulated data. Fig 4.8 gives a graphical overview of LSPC: for large Ns the pressure values do not match Van der Waal curves: more frames would have been required. Additionally, such plots confirm the prediction factor a was null, as the y intercept of the linear fits (Fig 4.5 & 4.6) is zero.

V. Conclusion

The aim of the simulation was to investigate multiple microscopic and macroscopic properties of gases, and it was successfully achieved.

However, it must be noted more powerful engines, capable of running more frames, would have obtained more accurate results in the computation of pressure for large numbers of balls and the subsequent fitting of Van der Waal equation of state.

VI. References

[1] Colling D, Paterson C, MacKinnon A. Computing Script. Project B: Thermodynamics Snookered. Sep 2016. Revised by Kingham R, Oct 2020.

[2] Freedman, D., Diaconis, P. On the histogram as a density estimator: L_2 theory. Probability Theory and Related Fields. 57, 453–476 (1981). Available from https://doi.org/10.1007/BF01025868.

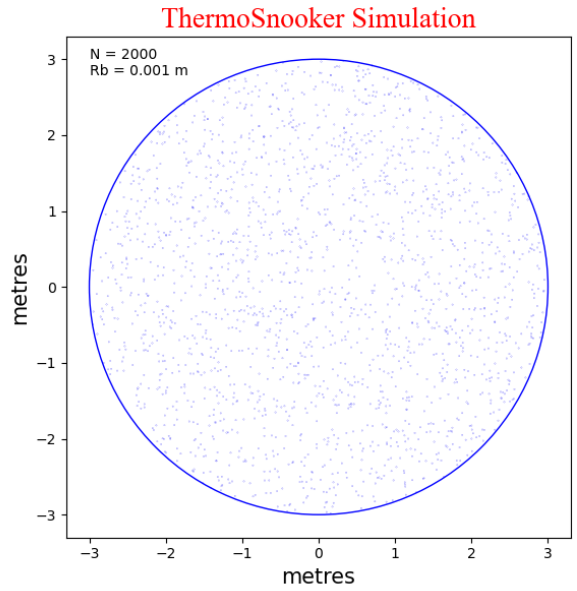

Figure 1.1 The simulation used for section II investigations.

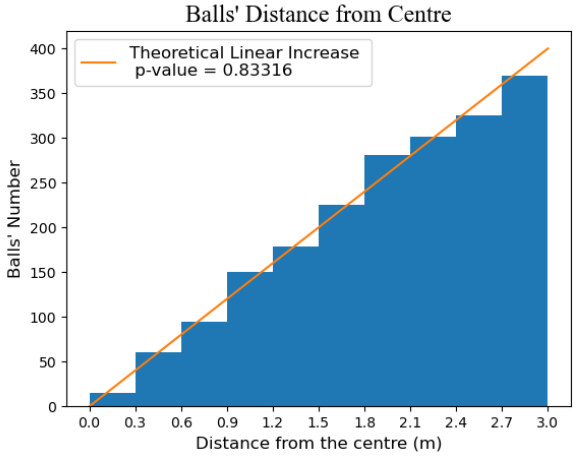

Figure 2.1 The distribution of the balls' distances form the centre of the container. As it can be seen, it increases linearly. The very high probability value of the chi squared test of the fit is displayed.

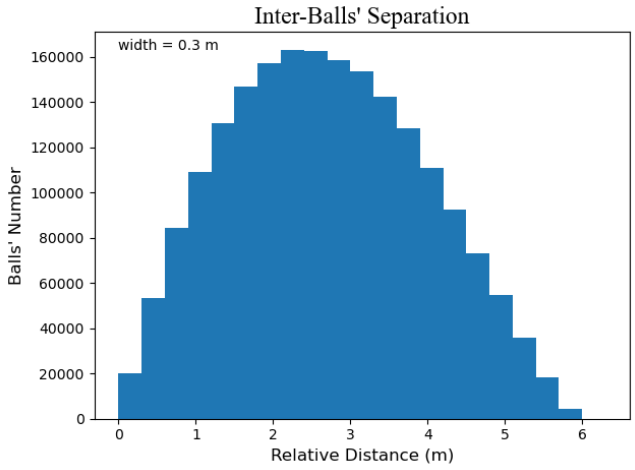

Figure 2.2 shows the distribution of the separation between the balls. The total number of distances for this is N(N-1)/2. For N = 2000, that means 1,999,000 cases.

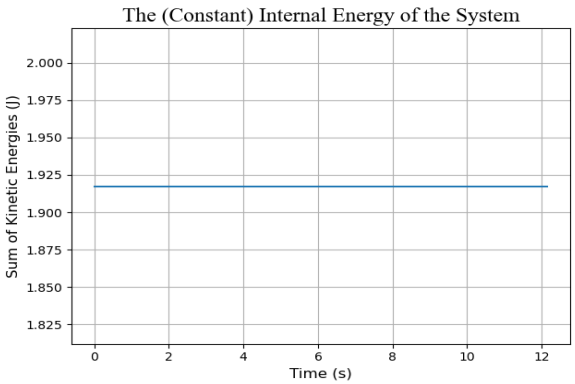

Figure 2.3 The total kinetic energy of the system is conserved.

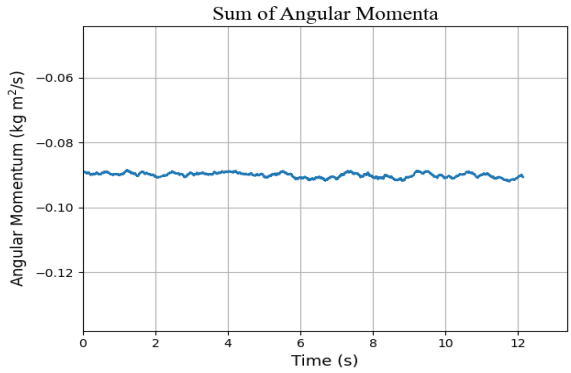

Figure 2.4 The total angular momentum is conserved, net of some floating-point imprecisions.

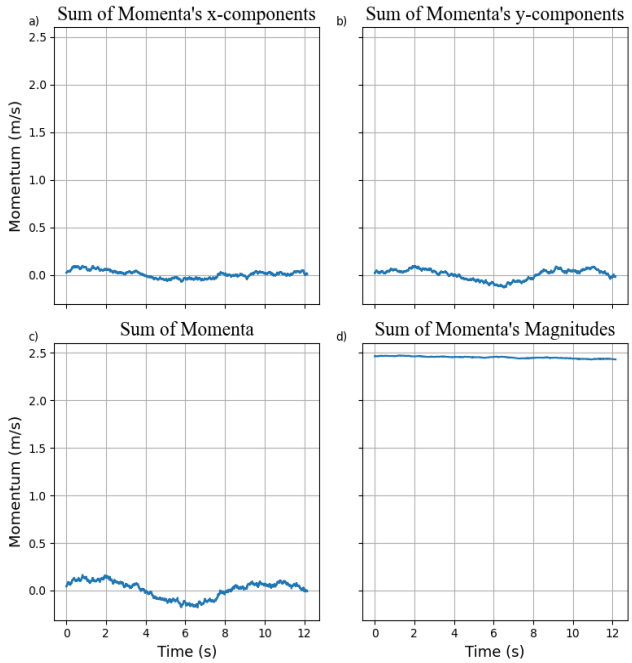

Figure 2.5 As it can be seen in plots a, b, c, momentum slightly oscillates as, when a ball bounces against the wall, its radial velocity is reversed (and also due floating-point imprecisions). Plot d shows the overall magnitude of momentum is conserved, net of some floating-point oscillations.

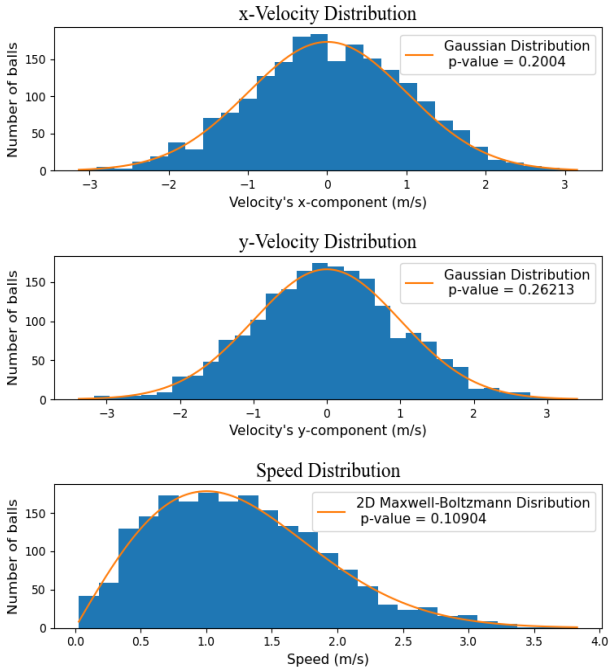

Figure 2.6 In the first two plots, the 0-centred gaussian distribution of velocities can be appreciated. In the last plot, the Maxwell-Boltzmann distribution of the speed is displayed. The high probability values of the chi squared tests for the fits are displayed.

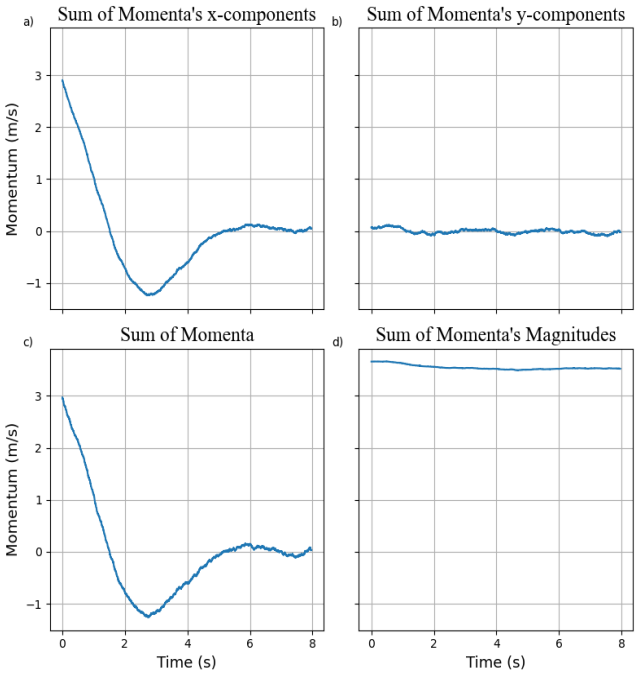

Figure 2.7 The plots are analogous to Fig 2.5 with the difference a boost in the x direction was initially supplied. The velocities tend to equilibrium anyways, as it can be seen.

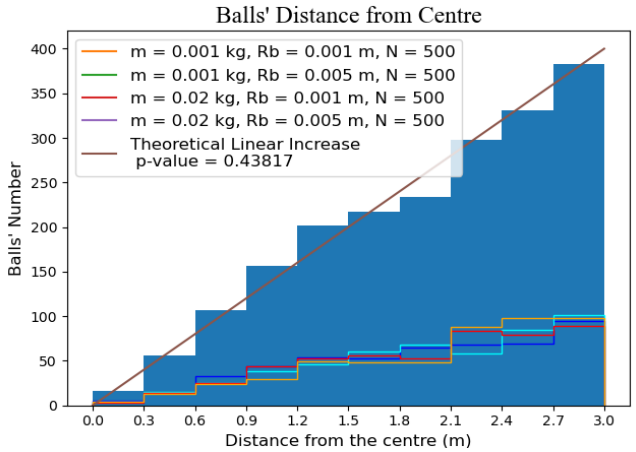

Figure 3.1 The distribution of the distance from the centre of the balls is independent of their mass and radius and matches the theoretical prediction.

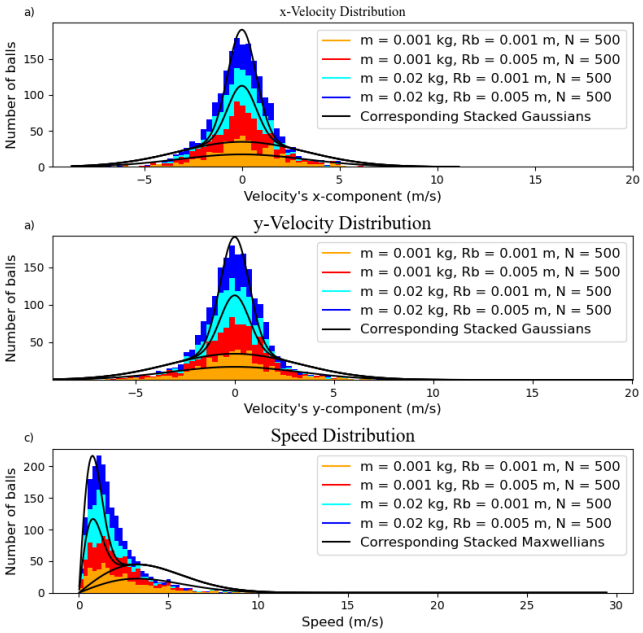

Figure 3.2 The distribution of the velocities follows the theoretical mass dependent prediction, even if not perfectly: I assume the discrepancy is caused by the smaller number of frames run (6000). The lighter particles have wider distributions.

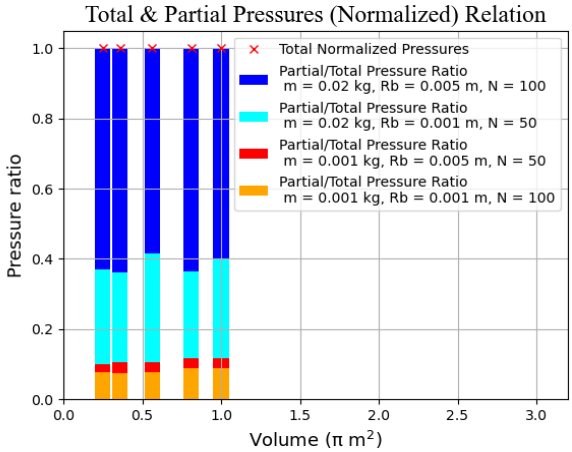

Figure 3.3. 5 simulations have been run for 5000 frames. The red xs have ordinate 1 by default. The coloured bars represent the ratio between the stacked partial pressures and the total pressure. As expected, their sum is equal to the total pressure itself (hence it is normalized in the plot). As it also was expected, the balls with bigger mass exerted bigger pressures.

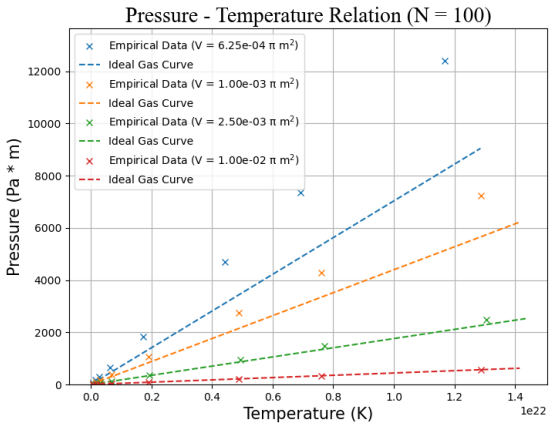

Figure 4.1 The PT linear relation for different volumes is displayed. It shows the inadequacy of the ideal gas equation.

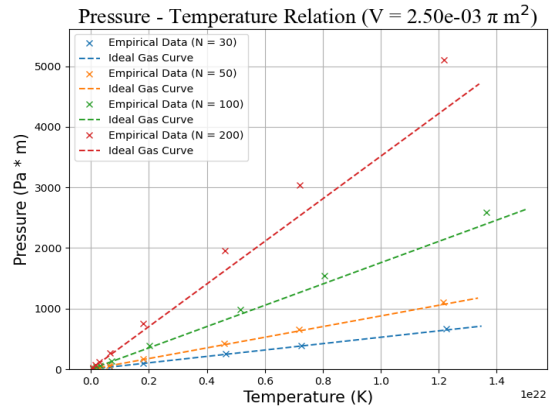

Figure 4.2 The PT linear relation for different Ns is displayed. It shows the inadequacy of the ideal gas equation.

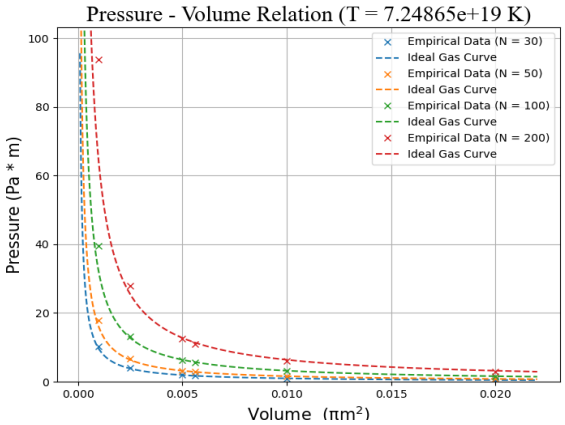

Figure 4.3 The PV inverse relation for different Ns is displayed. The ideal gas equation seems to be a reasonable fit here.

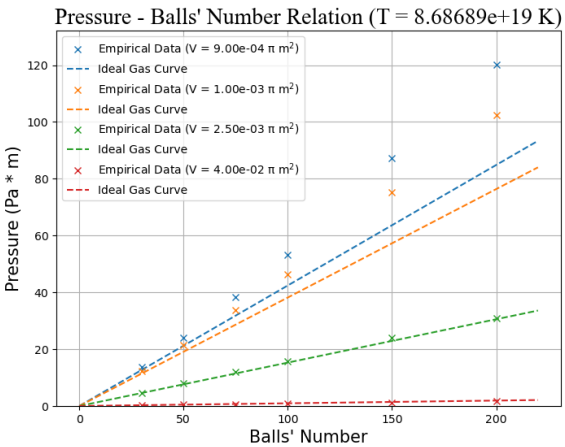

Figure 4.4 The PN relation for different volumes is displayed. It shows the inadequacy of the ideal gas model.

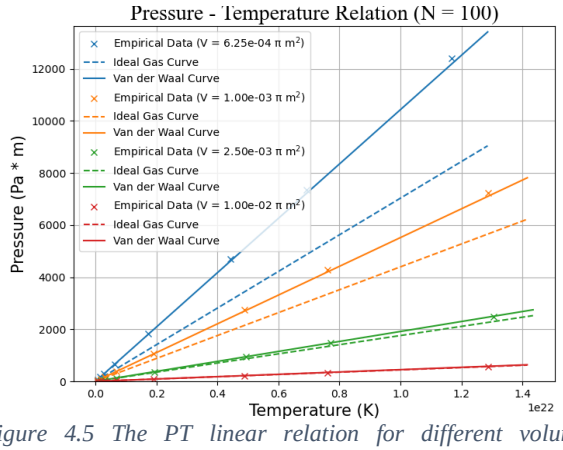

Figure 4.5 The PT linear relation for different volumes is displayed. It shows the superiority of Van der Waal model.

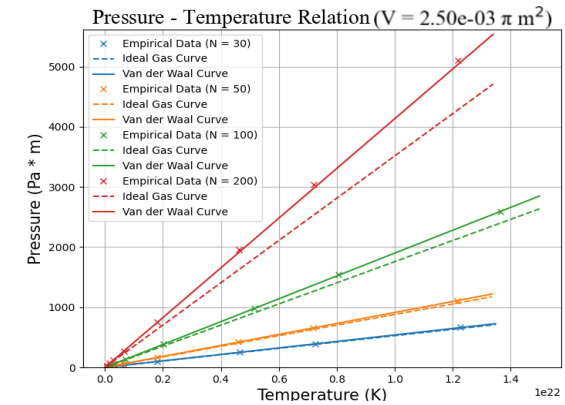

Figure 4.6 The PT linear relation for different Ns is displayed. It shows the superiority of Van der Waal model.

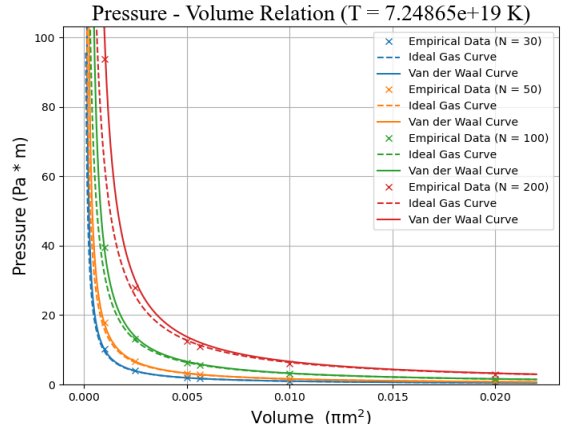

Figure 4.7 The PV inverse relation for different Ns is displayed. With less difference, it still confirms Van der Waal model.

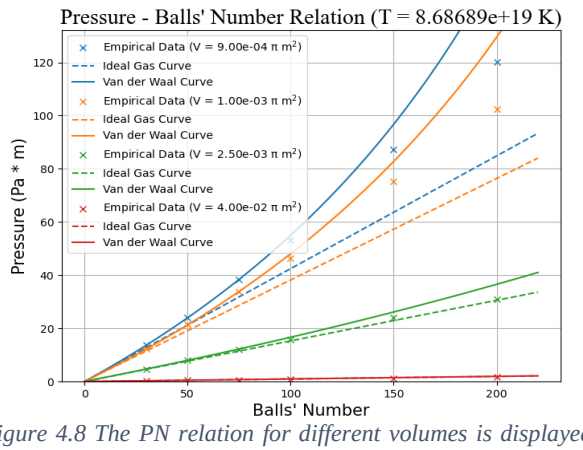

Figure 4.8 The PN relation for different volumes is displayed. As $N < 100$ Van der Waal clearly matches the data. As N is larger, the fit and data diverge, due to simulation's limitations (LSPC).